geoconvention
Calgary • Canada • May 12-14 2025

Attenuation of near-surface seismic waves with autoencoders

Ivan J. Sanchez-Galvis[1,2], Daniel O. Trad[1], William M. Agudelo[3], Daniel A. Sierra[2],
[1]CREWES – University of Calgary, [2]Universidad Industrial de Santander, [3]ECOPETROL S.A.,

Summary

Mask-based filters are widely used in seismic processing to isolate or enhance specific features in seismic data, such as reflections or diffractions, by suppressing undesired wave components such as Near-Surface Waves (NSW). However, defining these masks often relies on manual tuning, a process that is time-consuming, subjective, and prone to errors due to the complex and variable nature of seismic data. This limitation becomes particularly evident when processing data with overlapping signals or changing noise characteristics. To address these challenges, we propose two Machine Learning (ML) workflows that automate mask generation and improve the attenuation of NSW. The first workflow employs a finite-difference solver to create synthetic 3C seismic datasets with and without NSW, which are then processed using polarization analysis to train a U-Net autoencoder for mask prediction in the frequency-wavenumber (f, p) domain. The second workflow extends this approach by introducing a second U-Net autoencoder that refines the filtered seismic data in the time-offset (t, h) domain. These workflows were validated using synthetic datasets generated from the SEAM Foothills Phase II model. Results show that the trained models effectively reduce NSW, improving the clarity of deeper reflections in 3C seismic data. Future research will focus on applying these workflows to real datasets and incorporating diverse training scenarios to enhance model generalization.

U-Net autoencoder for NSW attenuation

U-Net is a specialized Convolutional Neural Network (CNN) designed for image segmentation, particularly in biomedical applications (Ronneberger et al., 2015). This architecture leverages convolutional layers to extract features and pooling layers to reduce dimensionality, producing compact latent representations. Unlike typical CNNs, U-Net integrates encoder-decoder components, with the decoder combining upsampled feature maps with contextual information from the encoder. This unique design facilitates precise segmentation even with limited training data by applying a tiling strategy to handle large images.

The U-Net has proven effective in separating seismic events in transformed domain panels using the Radon transform (Fontes et al.,2023). In this study, U-Net architecture is employed to detect NSW patterns in both the (f, p) and (t, h) domains. As illustrated in Figure 1, the input is a $64 \times 64 \times N_c$ 3D data array, where N_c denotes the number of channels. The architecture processed the input through four encoding levels using 3×3 convolutional layers and 2×2 max-pooling layers. It then decodes the data with similar layers, upsampling the latent representation. Finally, the output is produced through a 1×1 convolutional layer with a hyperbolic tangent activation function.

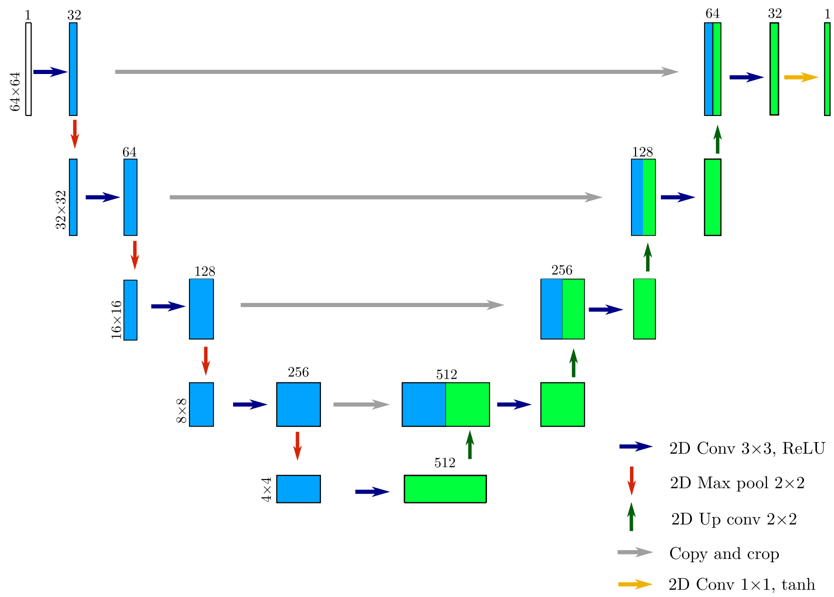

Figure 1. U-Net architecture for NSW attenuation.

To train the U-Net effectively, ground truth labels are essential for supervised learning. In this study, the objective is to predict 3C seismic data without NSW. However, direct processing in the (t, h) domain is often inadequate because high NSW amplitudes tend to obscure weaker body-wave reflections. To address this limitation, labels for filter masks are generated in the (f, p) domain using spectral elliptical elements (Sánchez-Galvis et al., 2024). The label $P_L(f, p)$ is defined as:

$$P_L(f,p) = \begin{cases} \dfrac{P_{DW}(f,p)}{P_{TW}(f,p)} & \text{if } P_L(f,p) > \varepsilon \\ 0, & otherwise \end{cases}, \tag{1}$$

where P_{TW} and P_{DW} are the power spectra for the total and deep wavefields, respectively, computed using the Partitioned Domain Method (PDM) introduced by Sánchez-Galvis et al. (2022). The constant ε ensures numerical stability by preventing division by zero. This filter mask design assigns lower values to regions dominated by NSW and higher values to regions where NSW is absent, thereby enabling accurate attenuation of NSW and enhancing the clarity of deeper reflections.

Machine Learning workflows

ML workflow in the frequency-slowness domain

The primary aim of this machine learning (ML) workflow is to predict a filter mask that can attenuate NSW in the $(f,\ p)$ domain. The training phase of this workflow comprises four key steps, as shown in Figure 2a. The first step involves computing synthetic data both with and without NSW by applying the PDM, which generates the total and deep wavefields. These data undergo a polarization analysis to derive the spectra of elliptical elements in the $(f,\ p)$ domain. These elements serve as inputs and attributes to generate labels for training the U-Net model architecture. Label generation utilizes equation (1), while inputs consist of the $(f,\ p)$ panels of semi-major axis a, semi-minor axis b, and azimuth of the ascending node Ω. These elements were chosen due to their superior performance, as reported by Sánchez-Galvis et al. (2024). The U-Net architecture, depicted in Figure 1, is then employed to predict the filter mask in the (f,p) domain.

For testing, the input is 3C seismic data, which is processed by polarization analysis to compute the spectra of elliptical elements. The elements (a, b, Ω) are subsequently fed into the trained U-Net model, which predicts the filter mask. This mask is then used to attenuate the NSW noise, yielding filtered 3C data. In this final stage, it is necessary to apply steps 4 and 5 of the procedure for polarization filtering outlined by Sánchez-Galvis et al. (2024).

Nested ML workflow

A nested ML workflow is proposed to enhance the results obtained from filtering in the (f,p) domain. This refined workflow builds on the outputs of the initial ML workflow by training a second autoencoder. In the first stage, the U-Net model predicts filter masks in the (f,p) domain using attributes from spectral elliptical elements. These filtered results are then used as inputs for the nested workflow, where the second autoencoder refines the data in the (t,h) domain. The second autoencoder uses the total wavefield as an additional input channel and the deep wavefield as its label. Importantly, the two autoencoders are trained independently, ensuring that the second model is robust to the initial filter's imperfections.

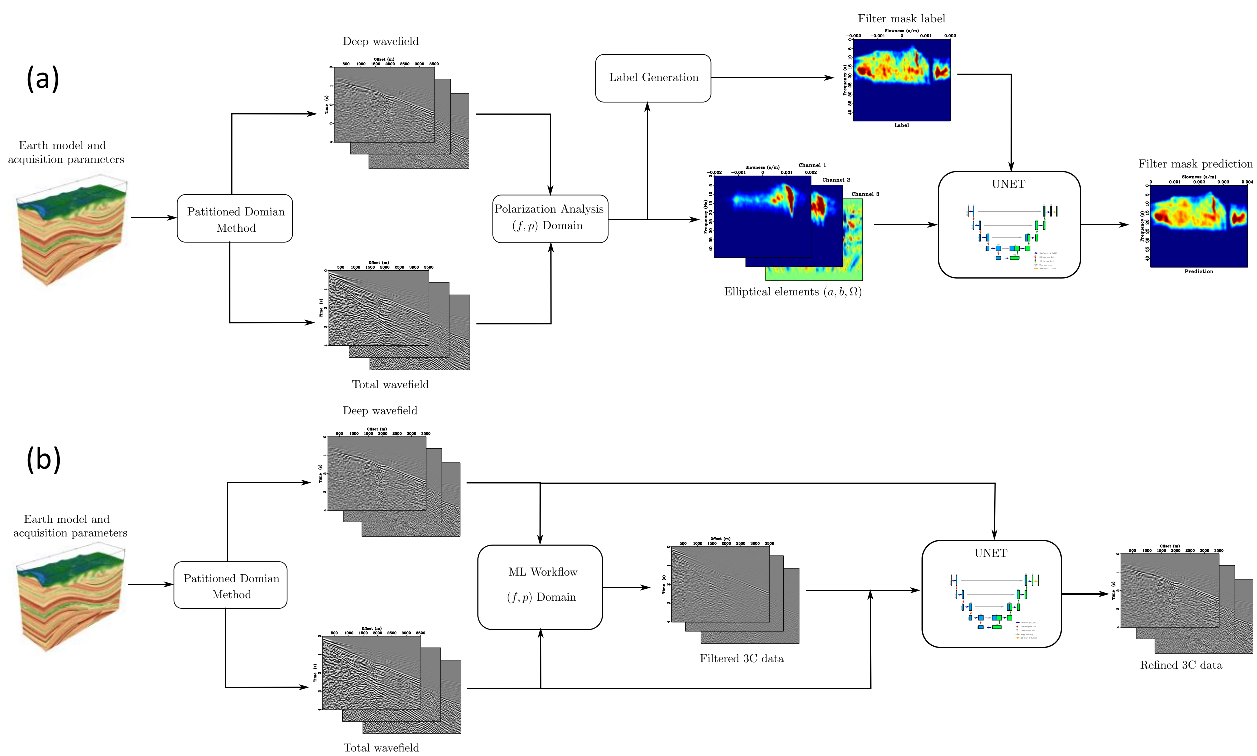

Figure 2. ML workflows for NSW attenuation. (a) Prediction of filter mask in the (f,p) domain. (b) Nested ML workflow in the shot domain.

Numerical test and results

The proposed ML workflows were trained and tested using synthetic datasets. These datasets consisted of 100 multicomponent shot gathers, generated using a section of the SEAM Foothills Phase II model whose topographic variation map shown in Figure 3. The acquisition geometry for each shot gather was consistent, with receiver lines placed along the x-axis from 500 to 5500 m, using an inter-receiver distance of 10 meters. The source was placed at $x = 2000$ m and $z = 12$ m. We produced 100 shot gathers by moving the acquisition geometry from $y = 500$ m to $y = 1500$ m in 10 m steps.

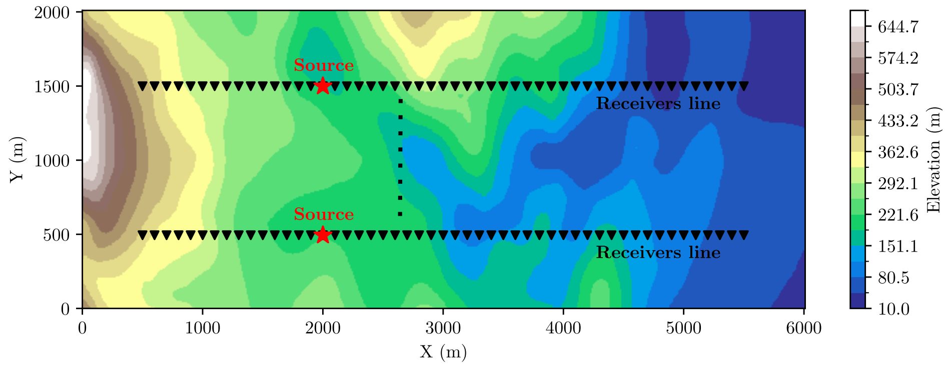

Figure 3. Elevation map and acquisition geometry for the portion of the SEAM model.

Synthetic data were generated with and without NSW by applying the PDM, and these data were fed into the ML workflows. During processing, the spectra of elliptical elements were computed to produce the U-Net model's inputs and labels. The inputs corresponded to the (f, p) panels of the semi-major, semi-minor, and azimuth of the ascending node, each serving as a channel input. A The training process utilized 80% of the dataset, with the remaining 20% used for validation. The label for this example was generated using the shot gather associated with the total wavefield and deep wavefield, as shown in Figures 4a and 4b, respectively. After the predicted filter mask was applied, most of the NSW was attenuated (see Figure 4c). However, the body-wave reflections remained weak. The application of the nested ML workflow enhanced the body-wave reflections, resulting in a greater visual similarity between the final output and the labeled deep wavefield (see Figure 4d), particularly for far offset.

Discussion and Conclusions

This study underscores the significant benefits of implementing ML workflows for attenuating NSW in 3C seismic data. In (Sánchez-Galvis et al., 2024), a 3C polarization filter was developed utilizing variable-parameter taper functions. However, the manual tuning of these functions is time-consuming and prone to human bias. Conversely, the proposed ML-based approach addresses these issues, offering a more efficient and objective method for the extraction of specific polarized energy. The numerical experiment with synthetic datasets showed that the U-Net autoencoder, trained with the PDM generated data, can accurately predict filter masks in the (f, p) domain. The ML workflow also includes a second autoencoder, further refining the filtered 3C seismic data in the (t, h) domain, thus demonstrating the feasibility of this approach in reducing NSW noise and enhancing the quality of deeper reflections.

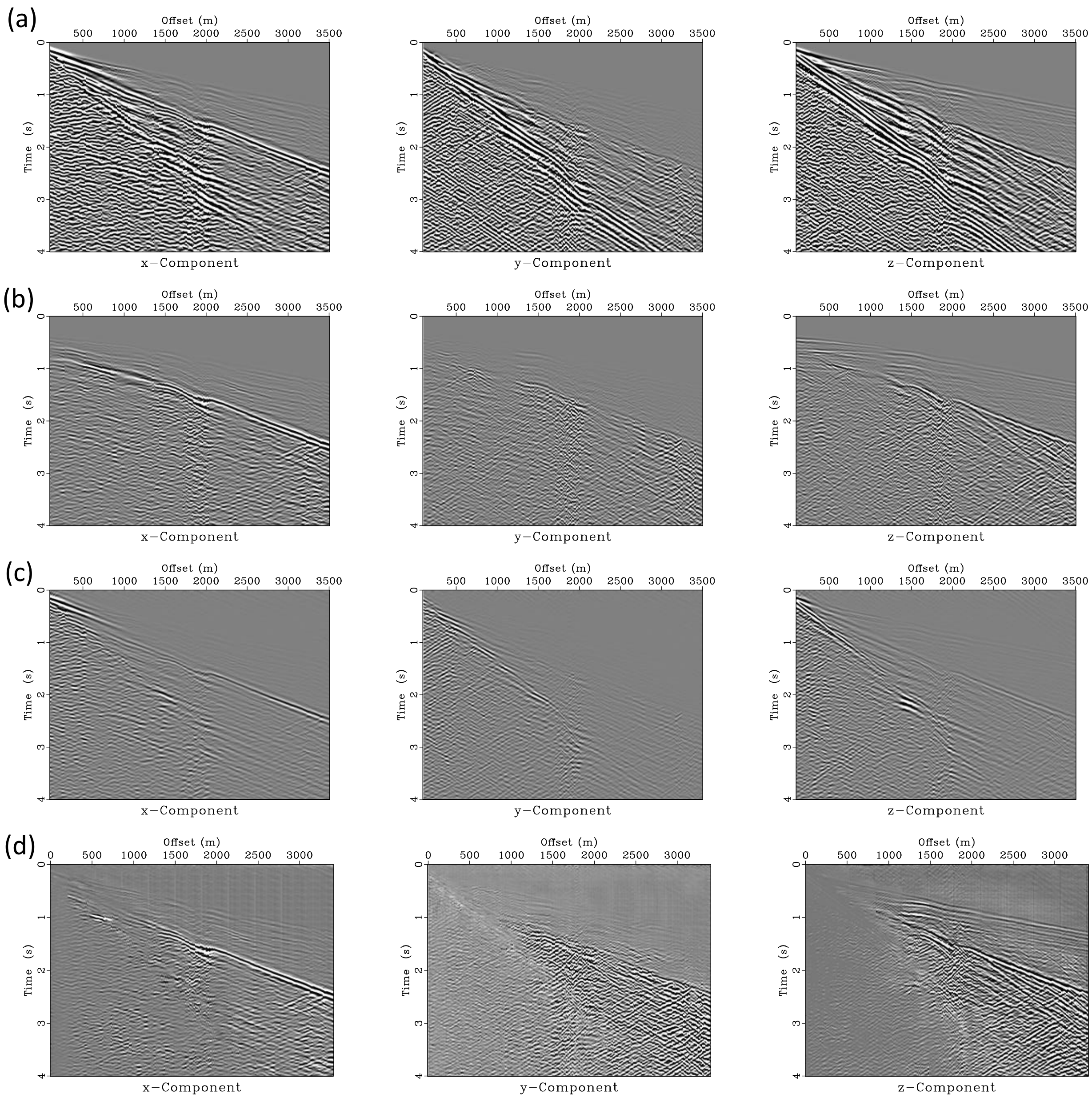

Figure 4. Multicomponent shot gathers inputs and outputs in machine learning workflows. (a) Input data. (b) Labeled output. (c) Output for ML workflow 1. (d) Output for ML workflow 2 (nested).

The ML workflows exhibited significant noise attenuation, enhancing the signal quality of deeper reflections. This highlights the robustness of ML algorithms in processing 3C seismic data and their capability to identify NSW patterns effectively. However, it is important to note that these workflows were trained exclusively on synthetic shot gathers generated from the SEAM Foothills Phase II model, which limits their generalization to real data applications. Future research should focus on incorporating datasets from diverse geological settings, including regions with low-velocity weathering layers or near-surface heterogeneities, to better represent variations in geological and noise conditions. Additionally, testing with real seismic acquisitions containing varying levels of noise contamination will be crucial for assessing and improving the model's robustness and generalization capabilities.

In conclusion, this study presented ML workflows as a promising new approach for attenuating NSW in 3C seismic data, offering substantial improvements over manual tunning approaches. While further research is needed to validate and optimize these workflows, the current results suggest a significant step forward in enhancing the quality and interpretability of 3C seismic data.

Acknowledgements

This work was funded by CREWES industrial sponsors and the Natural Science and Engineering Research Council of Canada (NSERC) through the grant CRDPJ 543578-19, with additional support provided by Emissions Reduction Alberta through the ACT4-SPARSE project. Furthermore, this research was conducted within the framework of the Agreement “Acta No. 27 del Convenio de Cooperación Tecnológica 5222395” between Universidad Industrial de Santander and Ecopetrol S.A.– Centro de Innovación y Tecnología ICP.

References

Fontes, P. H. L., Trad, D. O., & Sánchez-Galvis, I. J. (2023). The use of U-Net and hyperbolic Radon transform for multiple attenuation. In *GeoConvention, Conference Abstract*.

Ronneberger, O., Fischer, P., and Brox, T. (2015). U-Net: Convolutional networks for biomedical image segmentation. In International Conference on Medical image computing and computer-assisted intervention, pages 234–241. Springer.

Sánchez-Galvis, I. J., Agudelo, W., Trad, D. O., & Sierra, D. (2022). Simulated removal of near-surface scattered waves by elastic wave modeling. In *GeoConvention, Conference Abstract*.

Sánchez-Galvis, I. J., Agudelo, W., Trad, D. O., & Sierra, D. (2024). Polarization analysis and filtering of undersampled 3C seismic data in the frequency-slowness domain. *Geophysics*, *89*(5), 1-110.